

***M*-lines characterization of selenide and telluride waveguides for mid-infrared interferometry**

Lucas Labadie

Max-Planck Institut für Astronomie, Königstuhl 17, D-69117 Heidelberg, Germany
labadie@mpia.de

Laboratoire d'Astrophysique de l'Observatoire de Grenoble, BP 53, 38041 Grenoble Cédex, France

Caroline Vigreux-Bercovici and Annie Pradel

Laboratoire de Physico-Chimie de la Matière Condensée, Institut Gehrardt, UMR 5617, Place Eugène Bataillon, 34095 Montpellier Cédex 5, France

Pierre Kern and Brahim Arezki

Laboratoire d'Astrophysique de l'Observatoire de Grenoble, BP 53, 38041 Grenoble Cédex, France

Jean-Emmanuel Broquin

Institut de Micro-électronique et Photonique, UMR 5130, BP 257, 38016 Grenoble Cédex 1, France

Abstract: Nulling interferometry is an astronomical technique that combines equal wavefronts to achieve a deep rejection ratio of an on-axis star, and that could permit to detect Earth-like planets in the mid-infrared band [5 – 20 μm]. Similarly to what is done in the near-infrared, high frequencies spatial filtering of the incoming beams can be achieved using single-mode waveguides operating in the mid-infrared. An appreciable reduction of the instrumental complexity is also possible using integrated optics (IO) devices in this spectral range. The relative lack of single-mode guided optics in the mid-infrared has motivated the present technological study to demonstrate the feasibility of dielectric waveguides functioning at longer wavelengths. We propose to use selenide and telluride components to pursue the development of more complex IO functions.

© 2018 Optical Society of America

OCIS codes: (310.3840) Thin films; (120.4290) Instrumentation, measurement, and metrology

References and links

1. V. Coudé du Foresto, G. Perrin, J.-M. Mariotti, M. Lacasse, and W. Traub, "The FLUOR/IOTA fiber stellar interferometer," in *Proceedings of Integrated Optics for Astronomical Interferometry*, P. Kern and F. Malbet, eds. (Grenoble, France, 1997), pp. 115–125.
2. J.-P. Berger, P. Haguenaer, P. Kern, K. Perraut, F. Malbet, I. Schanen, M. Severi, R. Millan-Gabet, and W. Traub, "Integrated optics for astronomical interferometry. IV. First measurements of stars," *Astron. & Astrophys. Supp.* **376**, L31–L34 (2001).
3. F. Malbet, J.-P. Berger, P. Garcia, P. Kern, K. Perraut, M. Benisty, L. Jocou, E. Herwats, J.-B. Lebouquin, P. Labeye, E. Le Coarer, and O. Preis, "VITRUV - Imaging close environments of stars and galaxies with the VLTI at milli-arcsec resolution," presented at the VLTI Workshop on Optical and IR Interferometry, Garching bei München, Germany, 4–8 April 2005.

4. G. Perrin, J. Woillez, O. Lai, J. Guérin, T. Kotani, P. L. Wizinowich, D. Le Mignant, M. Hrynevych, J. Gathright, P. Léna, F. Chaffee, and S. Vergnole, "Interferometric coupling of the Keck telescopes with single-mode fibers," *Science* **311**, 194 (2006).
5. C. V. M. Fridlund, "The Darwin mission," *Adv. Space Res.* **34**, 613–617 (2004).
6. R. N. Bracewell, "Detecting non-solar planets by spinning infrared interferometer," *Nature (London)* **274**, 780–781 (1978).
7. J. R. P. Angel, A. Y. S. Cheng, and N. J. Woolf, "A space telescope for infrared spectroscopy of earth-like planets," *Nature (London)* **322**, 341–343 (1986).
8. B. Mennesson, M. Ollivier, and C. Ruilier, "Use of single-mode waveguides to correct the optical defects of a nulling interferometer," *J. Opt. Soc. Am. A* **19**, 596–602 (2002).
9. P. Bordé, G. Perrin, A. Amy-Klein, C. Daussy, and G. Mazé, "Updated results on prototype chalcogenide fibers for 10 μm wavefront spatial filtering," in *Proceedings of DARWIN/TPF and the Search for Extra-solar Terrestrial Planets*, M. Fridlund and T. Henning, eds. (Noordwijk, Netherlands, 2003), pp. 371–374.
10. U. J. Wehmeier, M. R. Swain, C. Y. Drouët D'Aubigny, D. R. Golish and C. K. Walker, "The potential of conductive waveguides for nulling interferometry," in *New Frontiers for Stellar Interferometry*, W. A. Traub, ed., Proc. SPIE **5491**, 1435–1443 (2004).
11. O. Wallner, V. G. Artjuschenko, and R. Flatscher, "Development of silver-halide single-mode fibers for modal filtering in the mid-infrared," in *New Frontiers for Stellar Interferometry*, W. A. Traub, ed., Proc. SPIE **5491**, 636–646 (2004).
12. L. Labadie, P. Labeye, P. Kern, I. Schanen-Duport, B. Arezki, and J.-E. Broquin, "Modal filtering for nulling interferometry – First single-mode conductive waveguides in the mid-infrared," *Astron. & Astrophys.* **460**, 1265–1266 (2006).
13. D. L. Lee, *Electromagnetic Principles of Integrated Optics* (John Wiley and Sons Ltd., 1986).
14. V. Kokorina, *Glasses for Infrared Optics* (CRC Press, 1996).
15. P. K. Tien, R. Ulrich, and R. J. Martin, "Modes of propagating light waves in thin deposited semiconductor films," *Appl. Phys. Lett.* **14**, 291–294 (1969).
16. P. K. Tien, "Light waves in thin films and integrated optics," *Appl. Opt.* **10**, 2395–2413 (1971).
17. H. J. Lee, C. H. Henry, K. J. Orlovsky, R. F. Kazarinov, and T. Y. Kometani, "Refractive-index dispersion of phosphosilicate glass, thermal oxide and silicon nitride films on silicon," *Appl. Opt.* **27**, 4104–4109 (1988).
18. J. M. White, and P. F. Heidrich, "Optical waveguide refractive index profiles determined from measurements of mode indices: a simple analysis," *Appl. Opt.* **15**, 151–155 (1976).
19. E. D. Palik, *Handbook of Optical Constants* (Academic Press New York, 1985).

1. Introduction

In the last ten years, the photonics field has provided a number of valuable technological solutions to astronomers to improve the performance of the observatories instruments. In particular, optical fibers and integrated optics (IO) devices have already been part [1, 2], or will be part in the future [3, 4] of interferometric facilities. As a result, this context has raised the question of extending the use of photonics devices to the Darwin Infrared Space Interferometer of the *European Space Agency* (ESA) [5].

This mission, based on the implementation of nulling interferometry [6], is devoted to the search and characterization of terrestrial exoplanets in the mid-infrared range thanks to its combined high contrast and high spatial resolution (long-baseline interferometry) features [7]. The principle of a two aperture nulling interferometer is to recombine artificially π phase-shifted wavefronts from an on-axis star in order to achieve their mutual cancellation. The signal from an off-axis object – like a planet orbiting the star – is transmitted through the instrument by tuning the interferometer baseline so that a total phase shift of 2π is achieved. A key requirement of nulling interferometry is equal wavefronts. Reducing the wavefront errors (e.g. pointing errors, optical defects due to polishing and coatings) can be obtained with single-mode waveguides as modal filters [8]. Using single-mode Integrated Optics (IO) components merges the functions of modal filtering and beam combination, providing a stable and compact instrument with regards to external mechanical and thermal constraints. To date, the implementation of modal filtering with single-mode waveguides has become the major option for space-based nulling interferometry.

The lack of single-mode waveguides for the mid-infrared in the photonics field has pushed

advanced technological studies to develop such devices [9, 10, 11]. In this context, we have initiated, under ESA contract, the *IODA* program (*Integrated Optics for DARwin*) to investigate the feasibility of a single-mode Integrated Optics concept operating over the full 5 – 20 μm spectral range. Our program has focused on the feasibility of an IO beam combiner based on either conductive waveguides [12] or on dielectric materials.

In this paper, we present results obtained using selenide and telluride materials to manufacture planar waveguides for the mid-infrared range, the first step toward further efforts for the development of channel waveguides. We show that the modal behavior of the various structures can be experimentally investigated and assessed with the *m*-lines method, known in the visible and near-infrared range, and which we have successfully transferred to the mid-infrared range. To our knowledge, this paper presents the first study of the modal properties of selenide and telluride thick films at longer wavelengths.

2. Investigating the properties of slab waveguides through *m*-lines study

2.1. Short theoretical analysis on fundamental parameters

It is well known that a planar waveguide must fulfill the total reflection condition at the interface between film–substrate and film–superstrate [13], corresponding to $n_c > \max(n_{\text{sub}}, n_{\text{sup}})$ with n_c , n_{sub} and n_{sup} the refractive indices of the film, substrate and superstrate, respectively. To propagate at least one mode, the thickness d of an asymmetric planar waveguide must be greater than the cut-off thickness of the fundamental mode d_0 given, in a more general form, by:

$$d > d_m = \frac{m\pi + \arctan\left(g \frac{\sqrt{n_{\text{sub}}^2 - n_{\text{sup}}^2}}{\sqrt{n_c^2 - n_{\text{sub}}^2}}\right)}{k\sqrt{n_c^2 - n_{\text{sub}}^2}} \quad (1)$$

where $k=2\pi/\lambda$ is the wave vector, m the mode order starting from 0, and g a polarization factor with $g=1$ for TE polarization and $g=n_c^2/n_{\text{sub}}^2$ for TM polarization. Thus, the quantity d_m increases with the operating wavelength and also depends on the dispersion of the material. Here, we briefly evaluate from a simple theoretical approach the possibility to benefit of a single-mode planar waveguide over the full Darwin range (5 – 20 μm) using As_2Se_3 glass as the layer and As_2S_3 glass as the substrate. The superstrate is air. We assume that these materials are transmissive over the entire range of interest, neglecting possible absorption lines. We also consider only the case of TE polarization with $g=1$. We derive from the refractive indices of these bulk materials [19] a simple fit of the dispersion laws which are given, to a first approximation, by $n_c(\lambda) = -0.00605 \times \lambda + 2.85091$ and $n_{\text{sub}}(\lambda) = -0.0095 \times \lambda + 2.47128$ for As_2Se_3 and As_2S_3 respectively, with λ given in microns. The adopted models are justified by the fact that the refractive indices of these materials decrease almost linearly in the 5 – 20 μm range. Under those assumptions, we compute the cut-off thicknesses d_0 and d_1 for modes $m=0$ and $m=1$ and for $5 \mu\text{m} < \lambda < 20 \mu\text{m}$. The acceptable slab thickness d for single-mode behavior over our spectral band must comply with $d_0(20\mu\text{m}) < d < d_1(5\mu\text{m})$. However, since we found $d_0(20\mu\text{m}) = 2.903 \mu\text{m}$ and $d_1(5\mu\text{m}) = 2.577 \mu\text{m}$, the previous condition cannot be fulfilled. The wavelength λ_1 for which $d_0(\lambda_1) \leq d_1(5\mu\text{m})$ is found to be $\lambda_1 = 17.2 \mu\text{m}$. Thus, it theoretically exists a film thickness, e.g. $d = 2.54 \mu\text{m}$, for which a planar waveguide following these dispersion laws propagates the fundamental mode only over a 5 – 17 μm band, i.e. almost the full expected band.

We underline that this modal analysis is based only on the study of the opto-geometrical parameters of the waveguide and is thus sensitive to the numerical fit. To better constrain

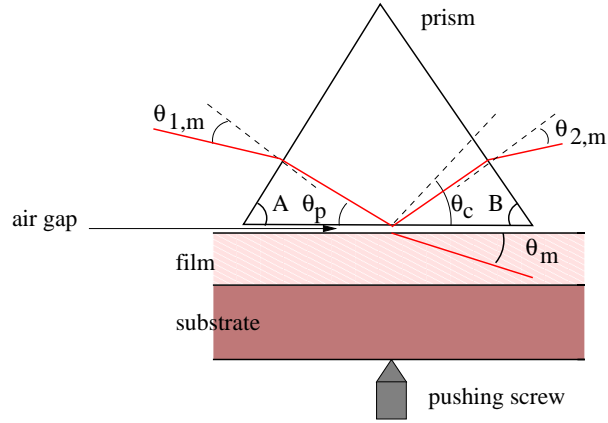


Fig. 1. Typical prism coupler setup. When we are in the condition of total reflection at the base of the prism (θ_p smaller than critical angle θ_c), the modes of the slab waveguide can be excited through the evanescent field existing in the air gap. The air gap thickness is controlled with a pushing screw at the back of the waveguide. A and B are the angles of the prism. $\theta_{1,m}$ and $\theta_{2,m}$ are the algebraic angles with respect to the normal of input and output prism facets corresponding to the excitation of mode m . θ_m is the angle of the propagating ray corresponding to mode m .

the trade-off between fundamental mode confinement and higher-mode filtering properties (which requires to be far from the cut-off), a more detailed electromagnetic approach through Beam Propagation Method (BPM) simulations will be required. However, our results show that a good compromise could reasonably be reached by splitting the $5 - 20 \mu\text{m}$ band into no more than two sub-bands, with two dedicated waveguide designs, and on the condition that a sufficient index difference between the film and the substrate is ensured.

2.2. Thick film deposition

Extending the IO solution to the mid-IR requires infrared materials with suitable features in this spectral domain. Chalcogenide glasses are interesting candidates, due to their good transparency in the mid-infrared, their high refractive index, and the relatively ease of preparation in films form. We have selected As_2Se_3 , $\text{Te}_2\text{As}_3\text{Se}_5$ and TeAs_4Se_5 chalcogenide compositions to undergo thick film deposition on an As_2S_3 substrate. Glasses containing elements like sulphur (S), selenium (Se) and tellurium (Te) transmit at longer wavelengths: sulphide glasses (i.e. As_2S_3) transmit up to $12 \mu\text{m}$, selenide glasses (i.e. As_2Se_3) transmit up to $16 \mu\text{m}$, and telluride glasses transmit up to $20 \mu\text{m}$ [14], with an average transmission of about 35% for the Te glass. Note that this transmission value includes the Fresnel losses at the interfaces due to the high refractive index of the glass. The deposition process used is thermal evaporation, which reduces the column-like effects in the structure and provides dense films with higher refractive index with respect to RF-sputtering techniques. The selenide films were deposited from As_2Se_3 commercial bulk glass, while the telluride films used bulk glass that was synthesized in the laboratory from commercial components like Tellurium (Te), Arsenic (As) and Selenide (Se).

The strategy adopted to develop the chalcogenide planar waveguides is the following. For both selenide and telluride compositions, we have selected As_2S_3 chalcogenide commercial glass as the substrate – the superstrate is air –, which presents the lowest refractive index among the different glasses available ($n=2.46$ at $\lambda=1.2 \mu\text{m}$ and $n=2.38$ at $\lambda=10 \mu\text{m}$). As under-

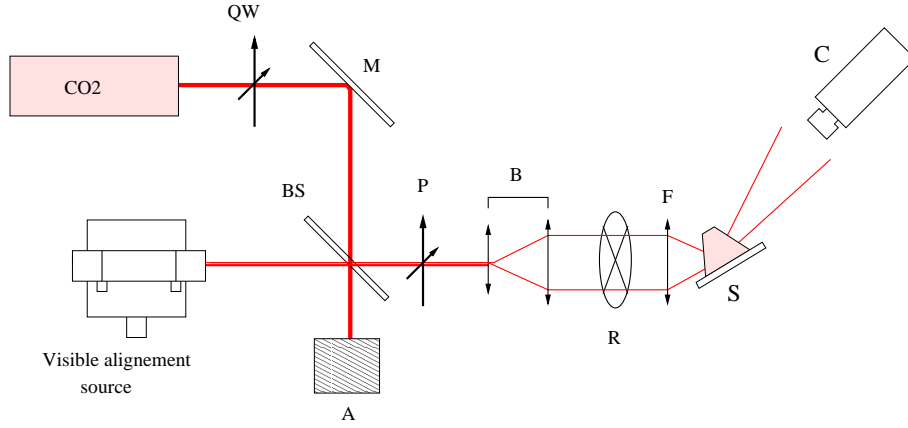


Fig. 2. Experimental arrangement of the mid infrared m -lines experiment: QW , quarter-wave plate; M , mirror; BS , beam-splitter; A , absorbing refractory brick; P , polarizer; B , beam-expander; R , reticle; F , focusing optics; S , system prism – film; C , infrared camera.

lined in Subsection 2.1, the challenge consisted in obtaining the appropriate index difference $\Delta n = n_c - n_{\text{sub}}$ and thickness d in order to propagate at least one mode. Eq. (1) shows that, for a given Δn , d_m is proportional to λ . Thus, at longer wavelengths the target thickness must be significantly higher than the usual thicknesses ($\approx 0.5 \mu\text{m}$) deposited for near-IR applications. Because of the novelty of the manufactured samples, an unknown is put on the achievable index difference and thickness. Consequently, we have experimentally investigated the modal behavior of the sample, the refractive index and the thickness of the films through the mid-infrared m -lines experiment developed at LAOG (Laboratoire d'Astrophysique de Grenoble).

2.3. Experimental technique

The m -lines method, based on prism coupling theory, was first proposed by Tien *et al.* [15] and is commonly used as a characterization method for telecommunication components in the visible and near-infrared range. In this study, we have implemented this method at $\lambda=10.6 \mu\text{m}$. In this technique, a prism is brought in close contact to the surface of a planar waveguide. Using a pushing screw placed under the waveguide (see Fig. 1), a small and localized optical contact is created between the prism base and the film. This provides a thin air gap that should optimally be a quarter of the operating wavelength to maximize the coupling effect. When a ray reaches the base of the prism with an incident angle smaller than the critical angle defined by the prism index, it becomes totally reflected. However, the overlap of the evanescent fields in the air gap as predicted by electromagnetic theory [16] implies that light can be coupled into the waveguide similarly to a tunneling effect. The existing modes of the waveguide will be excited if the phase matching conditions given by Eq. (2) are fulfilled

$$n_p \cos(\theta_p) = n_c \cos(\theta_m) \quad (2)$$

where n_p and n_c are respectively the prism and the thick film indices, and θ_p and θ_m are the angular directions of the rays as illustrated in Fig. 1. Exciting the low-order modes of the structure requires a prism with higher index than the slab waveguide index. Under these conditions, and for the incident rays that fulfill the phase conditions, the coupling phenomenon will lead to the observation of "black lines" at discrete positions $\theta_{2,m}$ in the reflected beam pattern. These

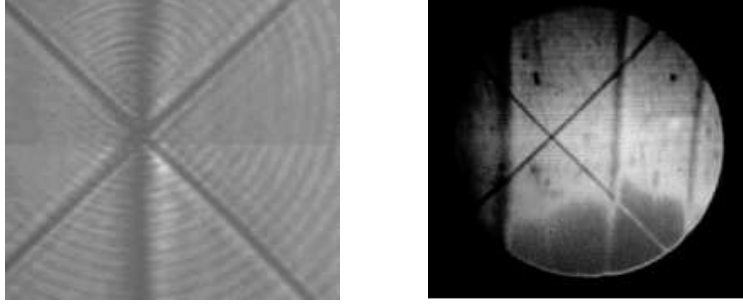


Fig. 3. Output of the m -lines experiment in the mid-IR (left) and in the near-IR (right). The image of the reticule is used to point the black lines by turning the prism stage. The mid-IR pattern presents a circular diffraction pattern due to the high coherence of the laser source.

lines are characteristic of the different modes of the slab waveguide. From the measurement of the angles $\theta_{2,m}$, the effective index $n_{\text{eff},m}$ of mode m is computed through:

$$n_{\text{eff},m} = n_p \sin \left(\arcsin \left(\frac{\sin(\theta_{2,m})}{n_p} \right) + B \right) \quad (3)$$

where B is one of the prism angles. The computation of the thick film index n_c and its thickness d is obtained by implementing a non-linear least squares method (see Subsection 2.4).

The experimental setup to measure the mode indices at $10.6 \mu\text{m}$ is shown in Fig. 2. The infrared source is a CO_2 laser. To probe either TE or TM modes, the quarter-wave plate QW modifies the intrinsic linear polarization of the source into an elliptical one, then the grid polarizer P selects the desired polarization. The Zinc Selenide (ZnSe) optics B and F produce a converging beam which is focused on the optical contact. This beam includes the angular directions that fulfill Eq. (2), simplifying the search for mode lines. The reticule is used to align the normal of the input face of the prism with the optical axis of the bench in order to solve Eq. (3). The black lines in the reflected beam are observed with a mid-infrared camera (see Fig. 3).

For the experiment at $10.6 \mu\text{m}$, we used a high-index germanium prism with an angle $B=30^\circ \pm 0.01^\circ$ and a refractive index $n_p=4.0 \pm 0.001$. In one case, the m -lines experiment was run at shorter wavelengths ($\lambda=1.196 \mu\text{m}$) and for which we used a silicon prism with an angle $B=44.8416^\circ \pm 5 \times 10^{-4}$ and a refractive index $n_p=3.5193 \pm 10^{-4}$. In our system, the position of the black line is measured with an accuracy of $\pm 0.01^\circ$.

2.4. Data processing

In this paper, we have assumed that the tested samples are asymmetric slab waveguides (i.e. $\text{Air}/\text{As}_2\text{Se}_3/\text{As}_2\text{S}_3$) with a step index distribution. To obtain a correct numbering of the modes, we used the property of linearity between the squared spectrum of mode indices $n_{\text{eff}}^2(m)$ and the mode numbers set $(m+1)^2$, as formalized by Lee *et al.*[17]. Thus, when more than three experimental mode indices are available, their numbering is derived from the computation of the linear regression coefficient ρ of the experimental curve $[n_{\text{eff}}^2(m), (m+1)^2]$ and compared to unity (see Tables 1,2). In this paper, we assume that mode numbering starts with $m=0$. Successively, we compute n_c and d by numerically solving [18] the waveguide dispersion equation for a step index distribution planar waveguide given by Eq. (4) [13]:

Mode	Measured angle	Angle separation	Experimental n_{eff}	Theoretical n_{eff}	Diff.
0	a	a	N/A	2.7729	N/A
1	a	a	N/A	2.7719	N/A
2	+25.65°	a	2.7697	2.7702	0.0005
3	+25.50°	+0.15	2.7682	2.7679	0.0003
4	+25.21°	+0.29	2.7654	2.7649	0.0005
5	+24.81°	+0.4	2.7614	2.7613	0.0001
6	+24.39°	+0.42	2.7573	2.7570	0.0003
7	+23.79°	+0.6	2.7513	2.7519	0.0006
8	+23.25°	+0.54	2.7459	2.7462	0.0003
9	+22.67°	+0.58	2.7400	2.7399	0.0001
Refractive index n_c		$2.7732 \pm 1.3 \times 10^{-4}$			
Thickness d		$13.74 \pm 0.05 \mu\text{m}$			

Table 1. TE mode indices obtained experimentally on sample **As-1** at $\lambda=1.196 \mu\text{m}$ with the m -lines setup. The error on the measured angle is $\pm 0.01^\circ$. The error on experimental n_{eff} is $\pm 1.3 \times 10^{-4}$. We found a maximum coefficient $\rho=-0.99923$ for the presented mode numbering. The silicon prism has $n_p=3.5193$ and $B=44.8416^\circ$. The substrate refractive index at $\lambda=1.196 \mu\text{m}$ is 2.47[19]. Note that the two first modes could not be experimentally observed with the silicon prism and are labelled as "a" for "absent". The sign "N/A" means "not applicable".

$$kd\sqrt{n_c^2 - n_{\text{eff},m}^2} - \arctan\left(g \frac{\sqrt{n_{\text{eff},m}^2 - n_{\text{sub}}^2}}{\sqrt{n_c^2 - n_{\text{eff},m}^2}}\right) - \arctan\left(g \frac{\sqrt{n_{\text{eff},m}^2 - n_{\text{sup}}^2}}{\sqrt{n_c^2 - n_{\text{eff},m}^2}}\right) = m\pi \quad (4)$$

To better constrain the result given by the linear regression coefficient method, we use the derived quantities n_c and d to compute the theoretical mode indices for different mode numbering by analytically solving Eq. (4). The correct mode numbering is then obtained through a best fit between the theoretical and experimental distributions of indices.

3. Results and discussion

3.1. Selenide components

The samples, with a target thickness around $10 \mu\text{m}$, were characterized in the near-IR ($\lambda=1.2 \mu\text{m}$) and in the mid-IR ($\lambda=10.6 \mu\text{m}$) with the m -lines setup presented in Subsection 2.3. Two samples were produced and respectively referenced as **As-1** and **As-2**. Sample **As-1** was characterized both at $\lambda=1.2 \mu\text{m}$ and at $\lambda=10.6 \mu\text{m}$, while sample **As-2** was characterized in the mid-IR only. Including the near-IR characterization is advantageous, since a multimode behavior is expected from the moment the film thickness is greater than $1 \mu\text{m}$. Thus, this increases the number of mode lines that can be detected and measured.

Table 1 reports the TE mode indices and the derived parameters for **As-1** at $\lambda=1.196 \mu\text{m}$. Sixteen mode lines were experimentally observed with the sample **As-1**, but only the first eight modes are presented here. Note that measurements of TM modes were not carried out because the two optical components QW and P in Fig. 2 were not available at the time of the corre-

sample As-1					
Mode	Measured angle	Angle separation	Experimental n_{eff}	Theoretical n_{eff}	Diff.
0	+55.04°	N/A	2.667	2.6666	0.0004
1	+46.89°	8.15	2.599	2.5992	0.0002
2	+36.09°	10.8	2.488	2.4868	0.0012
Refractive index n_c		2.689 ± 0.001			
Thickness d		13.27 ± 0.03 μm			
sample As-2					
0	+48.58°	N/A	2.614	2.6138	0.0002
1	+42.61°	5.97	2.557	2.556	0.001
2	+33.61°	9.00	2.4601	2.4606	0.0005
Refractive index n_c		2.633 ± 0.001			
Thickness d		14.49 ± 0.03 μm			

Table 2. TE mode indices obtained experimentally on samples **As-1** and **As-2** at $\lambda=10.6$ μm. The error on measured angle is $\pm 0.01^\circ$. The accuracies on prism index and angle lead to an error on experimental n_{eff} of $\pm 10^{-3}$. The maximum coefficient is $\rho=-0.99982$ for the given mode numbering. The prism has $n_p=4.00\pm 0.001$ and $B=30.0\pm 0.01^\circ$. The substrate refractive index at $\lambda=10.6$ μm is 2.38. The sign "N/A" means "not applicable".

sponding tests. Thus, only the intrinsic linear polarization of the source, corresponding to TE modes, was used for those two samples. The derived quantities are $n_c=2.7732 \pm 1.3 \times 10^{-4}$ and $d=13.74 \pm 0.05$ μm. A similar characterization was made at $\lambda=1.55$ μm, in order to observe a chromatic change in refractive index. This led to values $n_c(1.55\mu\text{m})=2.7407 \pm 1.3 \times 10^{-4}$ and $d=13.16 \pm 0.03$ μm. We observe a change in refractive index of approximately 0.04 as well as a small variation of the film thickness. Note that the m -lines experiment provides a measurement of the pair of quantities (n_c, d) for the film area where the optical contact is obtained. When shifting from $\lambda=1.2$ μm to $\lambda=1.55$ μm, we also moved the prism on the film, which has an effect on the measured film thickness.

We performed M -lines characterization in the mid-infrared at $\lambda=10.6$ μm for the two samples **As-1** and **As-2**. At longer wavelengths, the germanium prism described in Subsection 2.3 was used. Table 2 shows the experimental results obtained with the two samples. The value of the substrate index, $n_s=2.380$, has been taken from the literature [19].

For the two samples, three mode lines have been observed with our setup. The derived theoretical mode indices are very close to the experimental ones. The dispersion of the mode indices is low, which implies a good homogeneity of the index distribution. The derived refractive indices are $n_c=2.689 \pm 0.001$ for **As-1** and $n_c=2.633 \pm 0.001$ for **As-2**, which shows that the densification of the layer was lower during the second run. The sample thickness is approximately 13 μm for **As-1** and is consistent with the value obtained at shorter wavelengths. The thickness is slightly higher for **As-2** with a value of approximately 14.5 μm.

We measure mid-IR refractive indices significantly lower than in the near-IR. This is consistent with the dispersion law of the material, which predicts a decrease in the refractive index with increasing wavelength. We also note that the achieved thicknesses are greater than the targeted ones, which shows the deposition process needs to be better stabilized. Finally, a multimode behavior of the planar structures is clearly identified in the near and mid-IR ranges.

sample TAS-1 (TM polarization)					
Mode	Measured angle	Angle separation	Observed n_{eff}	Theoretical n_{eff}	Diff .
0	+55.83°	N/A	2.673	2.672	0.001
1	+43.56°	+12.27	2.567	2.561	0.006
2	+28.13°	+15.43	2.394	2.395	0.001
Refractive index n_c			2.709 ± 0.001		
Thickness d			10.72 ± 0.03 μm		
sample TAS-1 (TE polarization)					
Mode	Measured angle	Angle separation	Observed n_{eff}	Theoretical n_{eff}	Diff.
0	a	N/A	a	2.686	N/A
1	+45.26°	N/A	2.583	2.5887	0.0057
2	+30.13°	+15.13	2.419	2.4298	0.0108
Refractive index n_c			2.718 ± 0.001		
Thickness d			10.69 ± 0.03 μm		

Table 3. TM (up) and TE (down) mode indices obtained experimentally on sample **TAS-1** at $\lambda=10.6 \mu\text{m}$. The error on measured angle is $\pm 0.01^\circ$. The accuracies on prism index and angle lead to an error on experimental n_{eff} of $\pm 10^{-3}$. The same germanium prism as in Table 2 is used. The sign "a" means "absent" and "N/A" means "not applicable".

3.2. Telluride components

In this approach, the thick films were deposited by evaporation on a As_2S_3 substrate from $\text{Te}_2\text{As}_3\text{Se}_5$ and TeAs_4Se_5 bulk glasses made by LPMC (Laboratoire de Physico-chimie de la Matière Condensée). Two samples referenced **TAS-1** ($\text{TeAs}_4\text{Se}_5/\text{As}_2\text{S}_3$) and **TAS-2** ($\text{Te}_2\text{As}_3\text{Se}_5/\text{As}_2\text{S}_3$) were produced by thermal evaporation and characterized for TE and TM polarizations at $\lambda=10.6 \mu\text{m}$. The same germanium prism was used to achieve light coupling. The experimental measurements on **TAS-1** are reported in Table 3. For **TAS-2**, we present the derived refractive index and thickness only in Table 4. Mode lines have been observed for the two samples. The numerical analysis confirmed that the dark lines correspond to propagating modes. In this case as well, more than one line were observed.

For sample **TAS-1**, the fundamental mode in TE polarization could not be observed, oppositely to the TM case. For each mode, the measurement of the line angular position for the two polarizations was done successively. In this way, we could experimentally observe that there was a slight angular shift for the same mode between the two polarization. The m -lines measurement was done for TE and TM polarizations at the same point of the film. The results show a small difference between TM and TE index n_c , which supposes an hypothesis of birefringence of the film. For this first telluride component, an approximate thickness of the film of about $10 \mu\text{m}$ has been achieved.

The sample **TAS-2** was characterized with a similar procedure. Three mode lines have been experimentally observed but only in TE polarization. The corresponding TM case could not be observed despite our efforts in optimizing the coupling efficiency. For **TAS-2**, we therefore present the derived refractive index and thickness only in Table 4.

sample TAS-2 (TE polarization)					
Mode	Measured angle	Angle separation	Observed n_{eff}	Theoretical n_{eff}	Diff .
0	+73.59°	N/A	2.772	2.776	0.004
1	+52.45°	+21.14	2.647	2.640	0.007
2	+30.00°	+22.45	2.417	2.419	0.002
Refractive index n_c			2.821 ± 0.001		
Thickness d			8.79 ± 0.03 μm		

Table 4. TE mode indices obtained on sample **TAS-2** at $\lambda=10.6$ μm. The error on measured angle is $\pm 0.01^\circ$ and the accuracies on prism index and angle lead to an error on experimental n_{eff} of $\pm 10^{-3}$.

Compared to sample TAS-1, TAS-2 presents a higher refractive index at $\lambda=10$ μm. The possibility to obtain a high refractive index is an important result if a “full-telluride” (film and substrate) is foreseen. Using a telluride glass as a substrate will indeed raise the question of the achievable index difference between the film and the substrate, since telluride bulks are expected to present higher index compared to selenide bulks.

3.3. Impact of the experimental results on the requirements for single-mode slab waveguides

These experimental results show that the refractive index obtained with As_2Se_3 under thick film form is lower (by approximately 0.15) than in bulk form [19]. Since the index difference between the film and the substrate is an important parameter, we have now a less favorable case compared to the analysis of Subsection 2.1. Deriving the new model $n_c(\lambda) = -0.0127 \times \lambda + 2.78532$ from the data of Table 1 and 2, we find that we would need two $\text{As}_2\text{Se}_3/\text{As}_2\text{S}_3$ slab waveguides to cover the 5 – 20 μm band: the first one with a thickness $d=3.11$ μm for the sub-band 5 – 12.5 μm, and the second one with a thickness $d=7.0$ μm for the sub-band 12.5 – 20 μm.

Extending the first single-mode sub-band can be achieved with the telluride glass $\text{Te}_2\text{As}_3\text{Se}_5$ as the guiding layer, since the experimental results of Table 4 show that the achievable refractive index is higher than for As_2Se_3 .

However, the As_2S_3 substrate transparency remains an issue – it does not extend up to 20 μm. Therefore, covering the whole 5 – 20 μm band would require an examination of a 20 μm transparent telluride substrate, whose refractive index is sufficiently low to ensure a Δn of about 0.42.

4. Conclusions

This paper has discussed the optical characterization of chalcogenide-glass-based thick films manufactured for the purpose of future mid-IR integrated optics development. We have fully developed an m -lines setup operating at $\lambda=10.6$ μm based on prism coupling theory. This setup was used to characterize the modal behavior of the first mid-infrared planar waveguides by observing mode lines. In this study, two different compositions were successfully tested at 10 μm with the first observation of three mode lines for TE and TM polarizations. A simple numerical analysis based on a best fit between the experimental and theoretical mode indices distributions has permitted us to derive the refractive index and thickness of the different samples. Our results have underlined the possibility of producing full-selenide multimode planar waveguides with a sufficient film thickness. The near and mid-IR results are consistent, since similar thicknesses are obtained in the two spectral ranges. Extending the transmission range of the components to

20 μm may be possible with the telluride solution.

Following these results, a complementary technological study has been conducted to investigate the feasibility of a first full-telluride single-mode planar waveguide. This study has produced positive results. As a consequence, the question of etching of a channel waveguide to be used as a modal filter for nulling interferometry has been investigated straightforward and the results recently obtained will be part of a forthcoming paper.

Acknowledgments

This work was funded by European Space Agency contract 16847/02/NL/SFe, French Space Agency (CNES) and Alcatel-Alenia Space. The authors are grateful to Amal Chabli and Tom Herbst for useful discussions.